RESEARCH ARTICLE

KCNK1 inhibits osteoclastogenesis by blocking the Ca^{2+} oscillation and JNK–NFATc1 signaling axis

Jeong-Tae Yeon[1], Kwang-Jin Kim[2], Sang Woo Chun[3], Hae In Lee[3], Ji Yeon Lim[4], Young-Jin Son[2], Seong Hwan Kim[4],* and Sik-Won Choi[4],*

ABSTRACT

KCNK1 (K$^+$ channel, subfamily K, member 1) is a member of the inwardly rectifying K$^+$ channel family, which drives the membrane potential towards the K$^+$ balance potential. Here, we investigated its functional relevance during osteoclast differentiation. KCNK1 was significantly induced during osteoclast differentiation, but its functional overexpression significantly inhibited osteoclast differentiation induced by RANKL (also known as TNFSF11), which was accompanied by the attenuation of the RANKL-induced Ca^{2+} oscillation, JNK activation and NFATc1 expression. In contrast, *KCNK1* knockdown enhanced the RANKL-induced osteoclast differentiation, JNK activation and NFATc1 expression. In conclusion, we suggest that KCNK1 is a negative regulator of osteoclast differentiation; the increase of K$^+$ influx by its functional blockade might inhibit osteoclast differentiation by inhibiting Ca^{2+} oscillation and the JNK–NFATc1 signaling axis. Together with the increased attention on the pharmacological possibilities of using channel inhibition in the treatment of osteoclast-related disorders, further understanding of the functional roles and mechanisms of K$^+$ channels underlying osteoclast-related diseases could be helpful in developing relevant therapeutic strategies.

KEY WORDS: K$^+$ channel, KCNK1, Osteoclast, Ca^{2+}, JNK, NFATc1

INTRODUCTION

Each member of the two-P K$^+$ (K$_{2P}$) channels has two P loops and four transmembrane domains, and 15 mammalian genes in the family have been designated as genes encoding the K$_{2P}$ channels (*KCNK* genes) (Arrighi et al., 1998). Among them, K$_{2P}$1.1 (also called TWIK-1) is encoded by *KCNK1*. *KCNK1* is expressed in virtually all mouse tissues and its functional relevance has been documented in several tissues (Lesage et al., 1996, 1997; Arrighi et al., 1998; Enyedi and Czirjak, 2010). As a member of the inwardly rectifying K$^+$ channel family, KCNK1 drives the membrane potential towards K$^+$ balance potential, and it is expressed at significant levels in several tissues including heart, brain, pancreas, lung and placenta (Lesage et al., 1996, 1997; Arrighi et al., 1998). KCNK1 has been shown to contribute to a large passive K$^+$ conductance in rat hippocampal astrocytes, conduct inward leak Na$^+$ currents in human cardiac myocytes

under pathological hypokalemia, and regulate phosphate and water transport in mouse proximal tubule and medullary collecting duct (Nie et al., 2005; Zhou et al., 2009; Dempster et al., 2013), but its functional involvement in the process of osteoclast differentiation has not been well studied.

Overactivated osteoclasts increase the risk of fractures by weakening bones. This commonly occurs in several osteoclast-related diseases such as osteoporosis, Paget's disease, osteodystrophy, metastatic bone diseases and periodontal diseases (Cummings and Melton, 2002). The differentiation of hematopoietic stem cells into mature multinucleated osteoclast cells (MNCs) is basically regulated by two essential cytokines, macrophage colony-stimulating factor (M-CSF, also known as CSF1) and receptor activator of nuclear factor-κB ligand (RANKL, also known as TNFSF11) (Bucay et al., 1998; Boyce and Xing, 2008). Importantly, RANKL triggers signaling molecules that activate nuclear factor of activated T cells c1 (NFATc1), which subsequently regulates a number of osteoclast-specific genes, including tartrate-resistant acid phosphatase (TRAP, also known as ACP5), osteoclast-associated receptor (OSCAR), the d2 subunit of the V0 v-ATPase (ATP6V0D2) and cathepsin K (Rao et al., 1997; Takayanagi, 2007). RANKL also evokes Ca^{2+} oscillation, which in turn mediates NFATc1 expression and osteoclast differentiation.

In a preliminary study, DNA microarray analysis has revealed that *KCNK1* expression was increased by RANKL treatment in osteoclast precursors (data not shown). An increase of *KCNK1* expression from neonate to adult animals has also been shown (Arrighi et al., 1998), but its functional involvement in the process of osteoclast differentiation has not been reported to date. Therefore, herein, the relevance of *KCNK1* expression to the osteoclastogenesis was investigated through its gain-of-function and loss-of-function studies.

RESULTS

Increase of extracellular K$^+$ inhibits osteoclast differentiation

The effect of extracellular K$^+$ level on the RANKL-induced osteoclast differentiation was investigated in order to clarify the relevance of K$^+$ influx to osteoclast differentiation. Extracellular K$^+$ dose dependently attenuated RANKL-induced formation of TRAP$^+$ MNCs and TRAP activity (Fig. 1A–C) but not the survival of bone-marrow-derived macrophages (BMMs) (Fig. 1D).

KCNK1 mRNA and protein are gradually induced during osteoclast differentiation

The relevance of K$^+$ influx to osteoclast differentiation led us to investigate the genes involved in this process by DNA microarray analysis. When the gene expression levels in BMMs were compared to those in BMMs treated with RANKL for 1 day, a 1.5-fold increase of *KCNK1* was found to be induced by RANKL (data not shown). The gradual induction of *KCNK1* at its transcript and protein

[1]Research Institute of Basic Science, Sunchon National University, Suncheon 540-742, Republic of Korea. [2]Department of Pharmacy, Sunchon National University, Suncheon 540-742, Republic of Korea. [3]Department of Oral Physiology, College of Dentistry, Institute of Wonkwang Biomaterial and Implant, Wonkwang University, Iksan 570-749, Republic of Korea. [4]Laboratory of Translational Therapeutics, Pharmacology Research Center, Drug Discovery Division, Korea Research Institute of Chemical Technology, Daejeon 305-600, Republic of Korea.

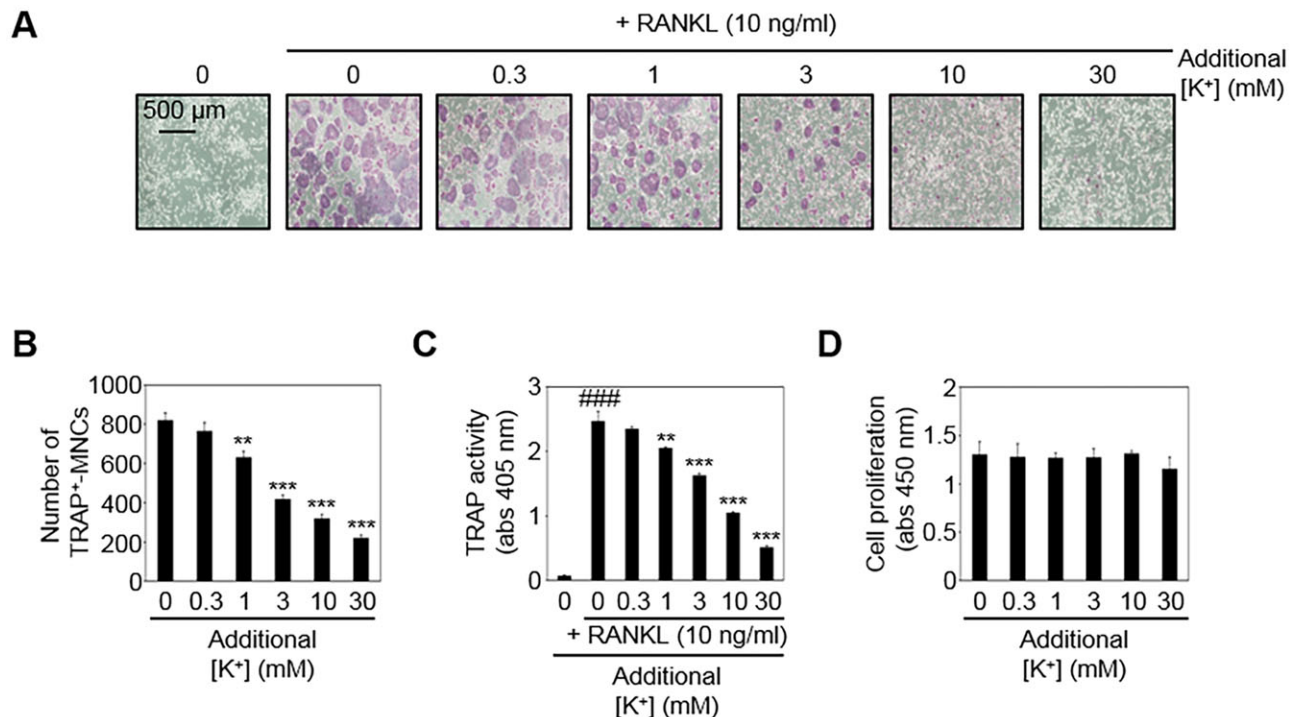*Authors for correspondence (hwan@krict.re.kr; superwon@krict.re.kr)

Fig. 1. Extracellular K$^+$ inhibits RANKL-mediated osteoclast differentiation. (A) BMMs were cultured for 4 days in the presence of RANKL (10 ng/ml) and M-CSF (30 ng/ml) with vehicle (PBS) or the additional K$^+$. Multinucleated osteoclasts were visualized by TRAP staining. (B) TRAP$^+$ MNCs were counted. **$P<0.01$; ***$P<0.001$ (versus the control). (C) TRAP activity was measured. ###$P<0.001$ (versus the control); **$P<0.01$; ***$P<0.001$ (versus the RANKL-treated group). (D) Effect of K$^+$ on the viability of BMMs was evaluated by a CCK-8 assay. All quantitative results are mean±s.d. (n=6).

expression levels during RANKL-induced differentiation of BMMs into osteoclasts was further verified by quantitative real-time PCR (qPCR) (Fig. 2A; supplementary material Fig. S1) and western blotting, respectively (Fig. 2B). Osteoclast differentiation was confirmed by evaluating the expression levels of molecules related to osteoclastogenesis including transcription factors, such as c-Fos, NFATc1, and/or its target molecules (TRAP, OSCAR, ATP6V0D2 and cathepsin K) (Jimi et al., 1999; Rao et al., 1997; Takayanagi et al., 2002; Takayanagi, 2007).

KCNK1 overexpression increases inward K$^+$ current

The functional relevance of KCNK1 to the osteoclast differentiation was investigated by a retrovirus-based gain-of-function experiment. Retroviral overexpression of *KCNK1* in BMMs was confirmed by quantitative reverse transcription PCR (qRT-PCR) (Fig. 3A). Furthermore, a patch-clamp experiment was carried out to evaluate whether overexpressed KCNK1 in BMMs acts functionally. As shown in the left graph of Fig. 3B, inward currents were significantly increased in KCNK1-overexpressing BMMs compared to the controls. An increase in amplitude of inward K$^+$ current following culture time was also observed (the right graph of Fig. 3B); the inward K$^+$ current exhibited a mean amplitudes of −274 ±59, −430±84 and −373±78 pA after a 1-, 2- or 3-day incubation with RANKL, respectively. Patch-clamp recording controls were performed using inward rectifying K$^+$ channel (Kir) blocker, Ba^{2+} (1 mM), and different concentrations of extracellular K$^+$ (supplementary material Fig. S2).

KCNK1 overexpression inhibits osteoclast differentiation

When KCNK1-overexpressing BMMs were cultured for 4 days with RANKL, the formation of TRAP$^+$ MNCs was strongly inhibited (Fig. 3C); the number of TRAP$^+$ MNCs and TRAP

activity were significantly attenuated by KCNK1 overexpression (Fig. 3D).

KCNK1 overexpression inhibits RANKL-induced JNK phosphorylation, expression of c-Fos and NFATc1 and intracellular Ca^{2+} oscillation

To gain insight into the mechanism by which KCNK1 overexpression inhibits osteoclast differentiation, its effects on the RANKL-induced activation of osteoclastogenesis-related early signaling molecules such as MAPKs and Akt were investigated. RANKL induced the phosphorylation of all kinases tested in this study, but KCNK1 overexpression was shown to attenuate the RANKL-induced phosphorylation of JNK (the isoforms p46 and p54 SAPK/JNK) (Fig. 4A).

Given that the RANKL-induced activation of JNK has been shown to subsequently lead to expression of transcription factors (Jimi et al., 1999; Srivastava et al., 1999; Shevde et al., 2000; Takayanagi et al., 2000), we further investigated the effect of KCNK1 overexpression on the expression levels of c-Fos and NFATc1, and their target genes such as *TRAP*, *OSCAR*, the v-ATPase d2 subunit and cathepsin K during osteoclast differentiation. RT-PCR revealed that *KCNK1* overexpression attenuated the RANKL-induced mRNA expressions of *c-Fos* and *NFATc1*, and their target genes (upper images in Fig. 4B). The attenuation of RANKL-induced protein expression of c-Fos and NFATc1 upon KCNK1 overexpression was also confirmed by western blot analysis (bottom images in Fig. 4B).

Intracellular Ca^{2+} oscillation has been reported to be required for the activation of c-Fos and NFATc1 during RANKL-induced osteoclast differentiation (Takayanagi et al., 2002; Sato et al., 2006). Noticeably, an attenuation of RANKL-induced Ca^{2+} oscillation upon KCNK1 overexpression in BMMs was also observed here (Fig. 4C).
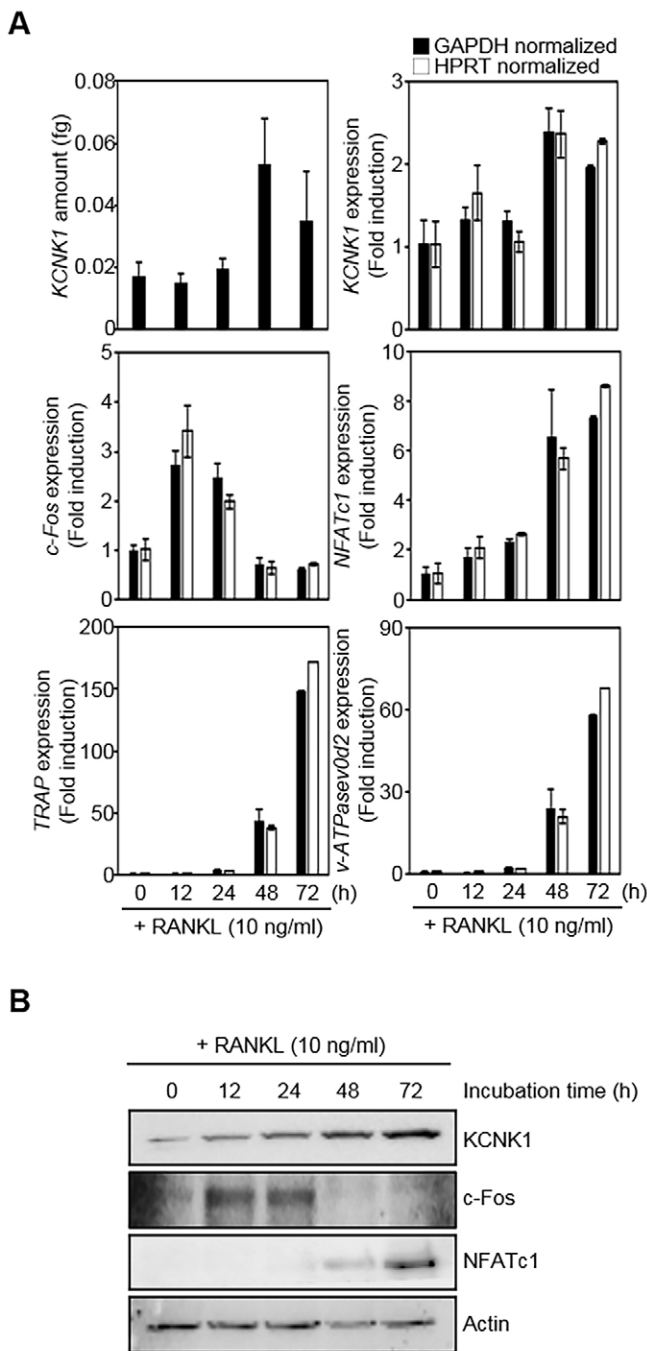
A

B

Fig. 2. KCNK1 induction during osteoclast differentiation. (A) When BMMs where differentiated into osteoclasts by RANKL (10 ng/ml) and M-CSF (30 ng/ml), the mRNA amount of *KCNK1* was quantified by comparison with DNA standard of *KCNK1* using a calibration curve (top in the left panel), and the relative mRNA expression levels of *KCNK1*, *c-Fos*, *NFATc1*, *TRAP* and the d2 subunit of V0 vATPase (*v-ATPasev0d2*) were measured by normalizing with those of two internal control genes, *GAPDH* and *HPRT*. (B) The protein expression level of *KCNK1* was measured by western blotting. Protein expression levels of osteoclastogenesis-related molecules were also evaluated. All quantitative results are mean±s.d. (*n*=3).

Increase of extracellular K⁺ inhibits intracellular Ca²⁺ oscillation

Given that KCNK1 mediates K$^+$ influx, in the condition of KCNK1 overexpression, higher K$^+$ influx might be expected. As with KCNK1 overexpression, extracellular K$^+$ also inhibited the

RANKL-induced JNK activation (Fig. 4D) and intracellular Ca^{2+} oscillation (Fig. 4E), suggesting that KCNK1-mediated K$^+$ influx can inhibit the RANKL-induced osteoclast differentiation by inhibiting JNK activation and intracellular Ca^{2+} oscillation.

KCNK1 knockdown reduces the inward K⁺ current

Using a retrovirus-based loss-of-function system, we further investigated the effect of *KCNK1* knockdown on the RANKL-induced osteoclast differentiation. qRT-PCR revealed the prominent inhibition of *KCNK1* mRNA expression in BMMs by its specific retroviral-transduced short hairpin RNA (shRNA) (upper images in Fig. 5A). Importantly, inward K$^+$ currents in BMMs were slightly reduced by the downregulation of *KCNK1* when compared to those of the control (bottom graph in Fig. 5A).

KCNK1 knockdown enhances RANKL-induced osteoclast differentiation, JNK phosphorylation, NFATc1 expression and the intracellular Ca²⁺ oscillation

In contrast to the effect of KCNK1 overexpression in the differentiation of BMMs into osteoclasts, the RANKL-induced formation of TRAP$^+$ MNCs was significantly enhanced by *KCNK1* knockdown (Fig. 5B,C). Furthermore, *KCNK1* knockdown enhanced the RANKL-induced phosphorylation of JNK (p46 and p54 SAPK/JNK), but not p38 MAPKs or ERK1/2 (Fig. 5D), and at the transcript and protein expression level, the induction of NFATc1 was also observed upon *KCNK1* knockdown (Fig. 5E).

KCNK1 knockdown nullifies the anti-osteoclastogenic action of extracellular K⁺

To investigate whether the enhancing effect of *KCNK1* knockdown on the RANKL-induced osteoclast differentiation overcomes the anti-osteoclastogenic action of extracellular K$^+$, the effect of K$^+$ on osteoclast differentiation was evaluated using *KCNK1*-knockdown BMMs. Consistent with the results shown in Fig. 1A and Fig. 5B, fewer TRAP$^+$ MNCs were formed in the presence of additional 3 mM K$^+$ (lower left image in Fig. 6A) and more TRAP$^+$ MNCs were formed after *KCNK1* knockdown (upper right image in Fig. 6A). Interestingly, there was no significant inhibition of osteoclast differentiation by K$^+$ in the condition of *KCNK1* knockdown (lower right image in Fig. 6A). The ability of *KCNK1* knockdown to reverse K$^+$-induced inhibition of osteoclastogenesis was confirmed by counting the number of TRAP$^+$ MNCs and measuring TRAP activity (Fig. 6B).

DISCUSSION

Several K$^+$ channels have been reported to be expressed in BMMs, the osteoclast precursors (Vicente et al., 2003), and the inwardly rectifying K$^+$ channel has been found in osteoclasts isolated from several species, indicating the presence of functional K$^+$ channels in osteoclasts (Sims and Dixon, 1989; Kelly et al., 1992). In addition, osteoclasts with a spread morphology, which represents a motile phase, have been shown to have an inwardly rectifying K$^+$ conductance, and rounded osteoclasts, which represent a resorptive phase of osteoclastic activity, have a transient, outwardly rectifying K$^+$ conductance (Arkett et al., 1992). Furthermore, the expression of Ba^{2+}-sensitive inwardly rectifying K$^+$ channels in the early phase of murine osteoclast differentiation has been suggested (Shibata et al., 1996).

Furthermore, the pharmacological possibilities of using K$^+$ channel inhibition to the treatment of osteoclast-mediated bone disorders has been recently suggested in several studies. The blockade of K$^+$ currents in mature osteoclast by charybdotoxin or
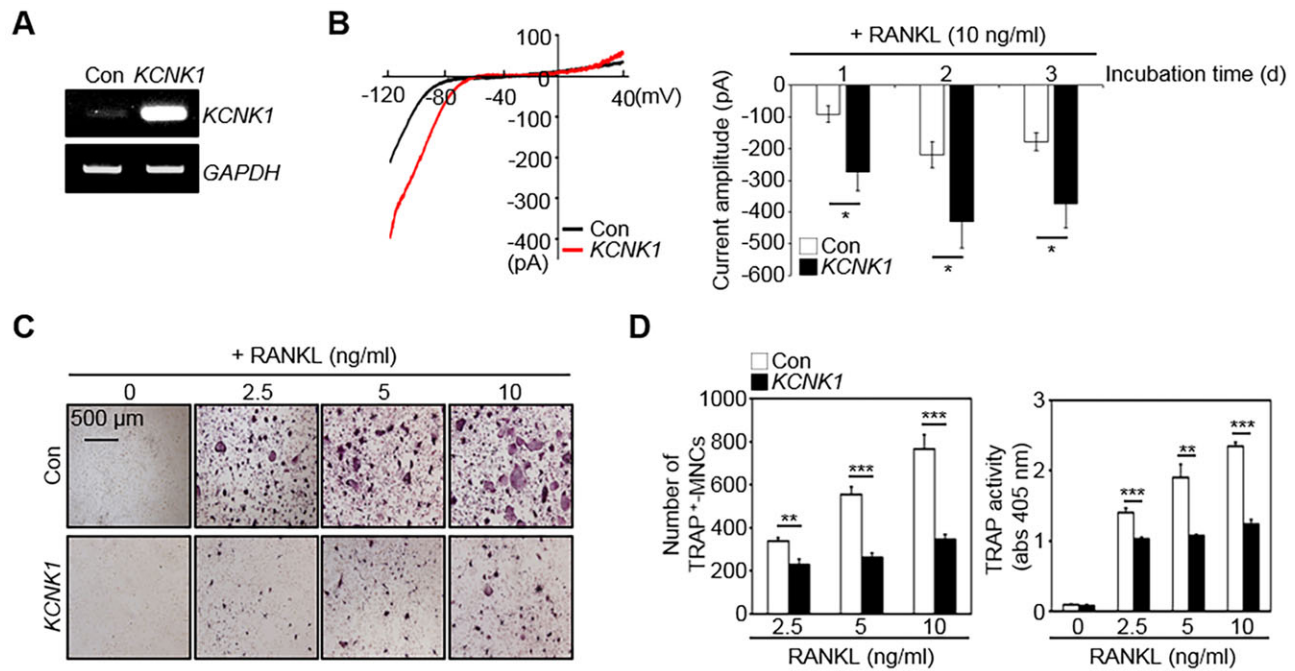
Fig. 3. KCNK1 overexpression inhibits RANKL-induced osteoclast differentiation. (A) BMMs were transduced with retroviruses harboring KCNK1 or pMX-Puro (the control), selected with puromycin (2 μg/ml) for 2 days, and cultured for 2 days in the presence of RANKL. Then, the mRNA level of KCNK1 was analyzed by qRT-PCR. The pMX-Puro-infected BMMs and KCNK1-overexpressing BMMs are presented as Con and KCNK1, respectively. (B) The current traces for cells as described in A were recorded at 20 mM of $[K^+]_o$ (left), and the amplitudes of the IKir were also measured after culturing cells for 1, 2 and 3 days in the presence of RANKL (right). *$P<0.05$ (versus the control). (C) In the presence of M-CSF (30 ng/ml), infected BMMs were differentiated into osteoclasts by treatment with RANKL for 4 days, and were then stained by TRAP solution. Mature TRAP+ MNCs were photographed under a light microscope. (D) TRAP+ MNCs and the TRAP activity were counted and measured. **$P<0.01$, ***$P<0.001$ versus the control. All quantitative results are mean±s.d. ($n=6$).

apamin (Ca^{2+}-activated K^+ channel blockers) has been shown to decrease the ability of osteoclasts to move and spread on bone substrate as well as to resorb bone (Espinosa et al., 2002), and kaliotoxin (a K^+ channel Kv1.3 blocker) can act to reduce inflammatory bone resorption in an experimental model of periodontal disease (Valverde et al., 2004). However, additional experiments are still required for validating the clinical application of K^+ channel blockers to treat osteoclast-mediated bone disorders (Valverde et al., 2005).

Here, we suggest that KCNK1 is a negative regulator of osteoclast differentiation; KCNK1 was gradually induced during osteoclast differentiation, but its overexpression, which induced an inward K^+ current in BMMs, strongly inhibited the RANKL-induced osteoclast differentiation, JNK activation and expression of c-Fos, NFATc1 and their target genes. In addition, KCNK1 overexpression inhibited the RANKL-induced Ca^{2+} oscillation. Considering that extracellular K^+ inhibited the osteoclast differentiation accompanied by the attenuation of RANKL-induced Ca^{2+} oscillation and JNK activation, these data suggest that KCNK1 could increase the influx of K^+ to inhibit osteoclast differentiation by attenuating the RANKL-induced Ca^{2+} oscillation and JNK activation that consequently downregulates NFATc1 expression. This suggestion was also confirmed upon the knockdown of KCNK1, and is supported by the following data.

The RANKL-evoked Ca^{2+} oscillation is well-known to trigger osteoclast differentiation through NFATc1 activation, which induces osteoclast-specific gene expression (Takayanagi et al., 2002; Yang and Li, 2007; Negishi-Koga and Takayanagi, 2009); the transient initial release of Ca^{2+} from intracellular stores and the influx through specialized Ca^{2+} channels controls the dephosphorylation of NFATc1 protein, and leads to its nuclear

localization, which is followed by the activation of osteoclast-specific genes. The importance of the RANKL–Ca^{2+}-oscillation–NFAT-activation signaling axis during osteoclast differentiation has been also confirmed by a pharmacological inhibition study where it was found that Ca^{2+} chelators inhibit the RANKL-induced osteoclast differentiation through suppressing of NFATc1 nuclear translocation (Negishi-Koga and Takayanagi, 2009). In addition, it has been suggested that intracellular Ca^{2+} levels and the activity of osteoclasts are reduced by the exposure to high K^+ (Kajiya et al., 2003). These data suggest that functional activation of K^+ channels might inhibit the RANKL–Ca^{2+}-oscillation–NFAT-activation signaling axis during osteoclast differentiation by increasing the influx of K^+.

As well as the RANKL–Ca^{2+}-oscillation–NFAT-activation signaling axis, the RANKL-induced activation of JNK is also essential for osteoclast differentiation (Darnay et al., 1998; Jimi et al., 1999; Kim et al., 1999; Srivastava et al., 1999; Shevde et al., 2000; Takayanagi et al., 2000; Chang et al., 2008). Activated JNK subsequently phosphorylates downstream factors, including c-Fos, which is required for NFATc1 induction. No evidence showing the relationship between exposure of high K^+ or inwardly rectifying K^+ channels and JNK activation during osteoclast differentiation had previously been provided, but here we suggest that the anti-osteoclastogenic activity of high K^+ and KCNK1 overexpression could attenuate RANKL-mediated activation of JNK.

In addition, when KCNK1 was induced by RANKL (which leads to several fold higher levels after 72 h incubation with RANKL), the cultures showed a large number of multinucleated osteoclasts. In contrast to the functional role of KCNK1 as a negative regulator of osteoclastogenesis, KCNK1 might also play a role as a positive
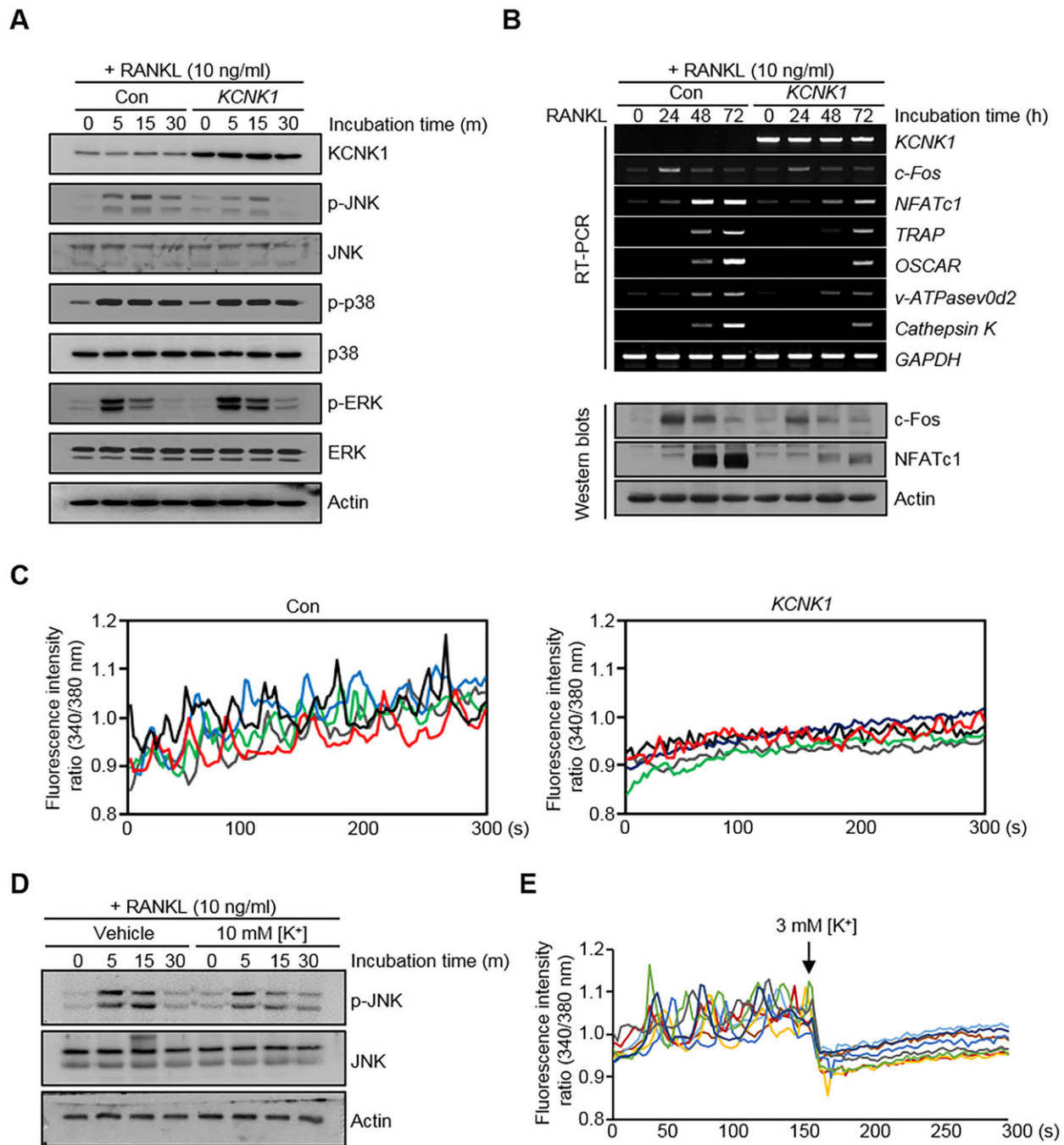
Fig. 4. KCNK1 overexpression and extracellular K+ attenuate RANKL-induced JNK activation and Ca2+ oscillation. (A) The pMX-Puro-infected BMMs and *KCNK1*-overexpressing BMMs are presented as 'Con' and '*KCNK1*', respectively. Both cell lines were cultured for 1 day in the presence of M-CSF and serum starved for 12 h and stimulated with RANKL (10 ng/ml) for the indicated times. Cell lysates were subjected to western blotting. (B) Infected BMMs were cultured with RANKL (10 ng/ml) for the indicated time in the presence of M-CSF (30 ng/ml), and then, the mRNA and the protein expression levels were analyzed by qRT-PCR and western blotting, respectively. The 'p-' prefix indicates the activate phosphorylated form of the protein. (C) Transduced BMMs were cultured in a black and clear-bottomed 96-well plate in the presence of RANKL (10 ng/ml) and M-CSF (30 ng/ml) for 2 days. After cells were incubated with 5 μM Fura-2-AM and 0.05% pluronic F127 for 30 min at room temperature, the fluorescence signaling were recorded at every 2–3 s with 340 and 380 nm excitations and emitted through a 510-nm cut-off filter using BD pathway system for 300 s. Each color indicates the results from a single cell. (D) After serum starvation for 2 h, BMMs were pretreated with vehicle or the additional K+ (10 mM) for 1 h prior to RANKL stimulation (10 ng/ml) for the indicated time periods. Protein levels were analyzed by western blotting. (E) In BMMs cultured with M-CSF and RANKL for 2 days, Ca2+ oscillation was recorded. After recording for 150 s, 3 mM [K+] was added. Ca2+ oscillation was recorded for the additional 150 s. Each color indicates the results from a single cell.

regulator to control the motility of mature osteoclasts (Arkett et al., 1992). Moreover, we suggest that the combined actions of ion channels, including KCNK1, with proton pumps could be necessary for the acidification and further bone resorption in mature osteoclasts, although further experiments are needed to substantiate this hypothesis.

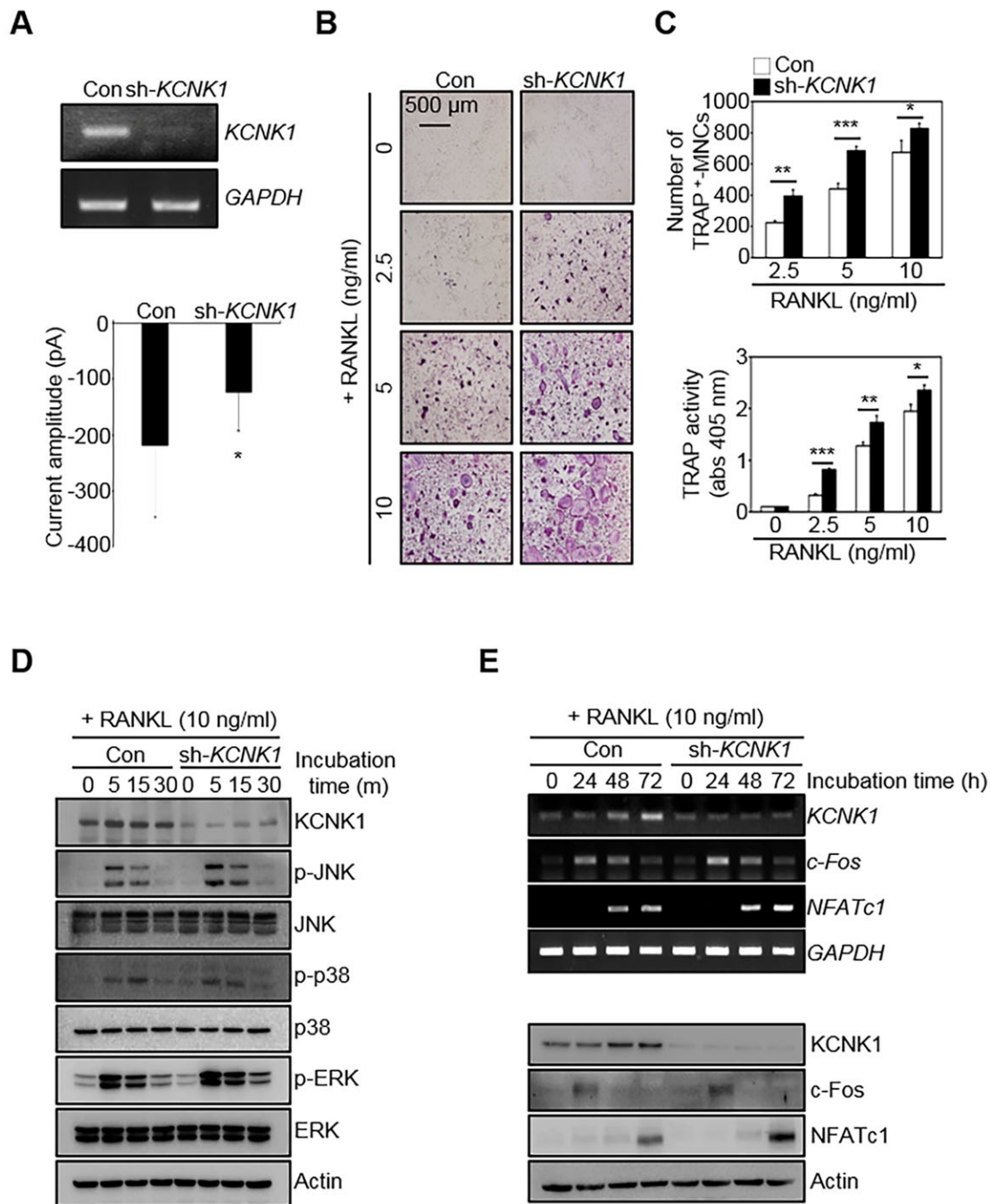In conclusion, we have determined that KCNK1 is a negative regulator of osteoclast differentiation through *in vitro*

Fig. 5. KCNK1 knockdown enhances RANKL-induced osteoclast differentiation. (A) BMM cells were infected with retroviruses encoding *KCNK1*-specific shRNA (sh-*KCNK1*) or pSuper-retro-puro (Con) and selected with puromycin (2 μg/ml) for 2 days. In infected BMMs cultured for additional 2 days, the mRNA expression of *KCNK1* was analyzed by qRT-PCR and the current traces were recoded using a patch-clamp system. *$P<0.05$. (B) In the presence of M-CSF, transduced BMMs were cultured with RANKL for 4 days and stained for TRAP. (C) Numbers of TRAP$^+$ MNCs were counted and TRAP activity measured. *$P<0.05$, **$P<0.01$, ***$P<0.001$ (versus the control). (D) After infected BMM cells were cultured for 1 day with M-CSF (10 ng/ml), serum-starved for 12 h, and stimulated with RANKL (10 ng/ml) for the indicated time. Then, protein expression levels were evaluated by western blot analysis. Actin was used as the internal control. The 'p-' prefix indicates the activate phosphorylated form of the protein. (E) Selected BMMs were cultured with RANKL for the indicated time. Then, the mRNA and protein levels were analyzed by qRT-PCR (upper panel) and western blotting (bottom panel). *GAPDH* or actin was used as the internal control in each assay. All quantitative results are mean±s.d. (*n*=6).

gain-of-function and loss-of-function studies; KCNK1 is gradually induced during osteoclast differentiation, but in KCNK1-overexpressing BMMs with the increase of inward K$^+$ current, the RANKL-induced osteoclast differentiation was significantly inhibited through the attenuation of the RANKL-induced Ca^{2+} oscillation, JNK activation and NFATc1 expression. Better understanding for the functional roles and mechanisms of K$^+$ channels underlying osteoclast-related diseases could be helpful to develop the relevant therapeutic strategy.
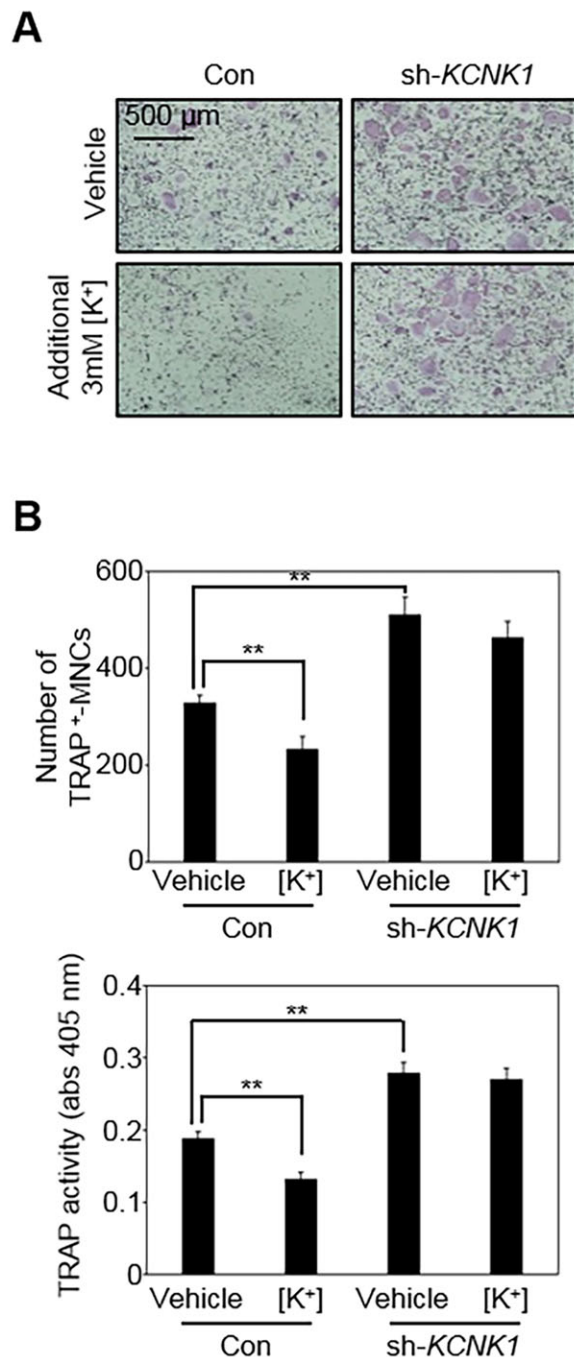
Fig. 6. *KCNK1* knockdown nullifies the anti-osteoclastogenic action of extracellular K⁺. (A) BMMs infected with retroviruses encoding *KCNK1*-specific shRNA (sh-*KCNK1*) or pSuper-retro-puro (Con) were cultured with RANKL (10 ng/ml) and M-CSF (30 ng/ml) for 4 days in the presence of the vehicle (PBS) or an additional 3 mM K⁺. Multinucleated osteoclasts were visualized by TRAP staining. (B) Numbers of TRAP⁺ MNCs were counted and TRAP activity measured. **$P<0.01$. All quantitative results are mean±s.d. (n=6).

MATERIALS AND METHODS
Osteoclast differentiation
This study was carried out in strict accordance with the recommendations in the Standard Protocol for Animal Study of Korea Research Institute of Chemical Technology (KRICT; No. 2012-7D-02-01). The protocol (ID No. 7D-M1) was approved by the Institutional Animal Care and Use Committee of KRICT. All efforts were made to minimize suffering. Five-week-old male

ICR mice (Damul Science Co., Deajeon, Korea) were maintained in a room illuminated daily from 07:00 to 19:00 (a 12-h-light–12-h-dark cycle) under controlled temperature (23±1°C) and ventilation (10–12 times per hour). Humidity was maintained at 55±5%, and the mice had free access to a standard animal diet and tap water. To isolate bone-marrow-derived cells (BMCs) from mice, after cervical dislocation, femur and tibia were flushed with α-MEM (Invitrogen Life Technologies, Carlsbad, CA) supplemented with antibiotics (100 units/ml penicillin and 100 µg/ml streptomycin; Invitrogen Life Technologies). BMCs were cultured on a culture dish in α-MEM (including 5.3 mM KCl) supplemented with 10% fetal bovine serum (FBS; Invitrogen Life Technologies) with 10 ng/ml of mouse recombinant M-CSF (R&D Systems, Minneapolis, MN) for 1 day. Then, after non-adherent BMCs were replated on a Petri dish and cultured for 3 days in the presence of M-CSF (30 ng/ml), adherent bone marrow-derived macrophages (BMMs) were used for osteoclast differentiation. For osteoclastogenesis, BMMs (1×10^4 cells/well in a 96-well plate or 3×10^5 cells/well in a six-well plate) were seeded in triplicate and cultured in the presence of 10 ng/ml of mouse recombinant RANKL (R&D Systems, Minneapolis, MN) and M-CSF (30 ng/ml) for 4 days to differentiate into mature TRAP-positive MNCs (TRAP⁺ MNCs).

TRAP staining and activity assay
Mature osteoclasts were visualized by staining for TRAP, a biomarker of osteoclast differentiation. Briefly, multinucleated osteoclasts were fixed with 3.7% formalin for 10 min, permeabilized with 0.1% Triton X-100 for 10 min, and stained with TRAP solution (Sigma-Aldrich, St Louis, MO). TRAP⁺ MNCs (≥3 nuclei) were counted. To measure TRAP activity, MNCs were fixed in 3.7% formalin for 5 min, permeabilized with 0.1% Triton X-100 for 10 min, and treated with TRAP buffer (100 mM sodium citrate pH 5.0, 50 mM sodium tartrate) containing 3 mM *p*-nitrophenyl phosphate (Sigma-Aldrich) at 37°C for 5 min. Reaction mixtures in the wells were transferred to new plates containing an equal volume of 0.1 N NaOH and the absorbance was determined at 405 nm.

Cell proliferation assay
BMMs were plated in a 96-well plate at a density of 1×10^4 cells/well in triplicate. After treatment with M-CSF (30 ng/ml) and various concentrations of K⁺, cells were incubated for 3 days. Then, cell viability was measured using the Cell Counting Kit 8 (CCK-8) according to the manufacturer's protocol.

RNA isolation and RT-PCR
According to the manufacturer's protocols, total RNA was isolated with TRIzol reagent (Invitrogen Life Technologies), and reverse transcription was performed with 1 µg of RNA using oligo(dT) primers, dNTP, RNase inhibitor and SuperScript II reverse transcriptase (Invitrogen Life Technologies). The cDNA was amplified using an i-Star Taq premix PCR kit (Intron Bio, Seongnam, Korea). The thermal cycling conditions consisted of 30 s denaturation at 94°C, 30 s anneling at 60°C and 30 s extenstion at 72°C. PCR products were electrophoresed on a 1% agarose gel stained with ethidium bromide. Supplemenatry material Table S1 lists primers used in this study. *GAPDH* and *HPRT* were used as an internal control. Additionally, SYBR-based real-time quantitative PCR was performed in triplicate to quantify by absolute quantification the exact amount of *KCNK1* mRNA by comparison with a DNA standard of *KCNK1* using a calibration curve.

Western blot
Western blotting was carried out as described previously (Choi et al., 2014). Briefly, cells were washed with ice-cold phosphate-buffered saline (PBS) and lysed in lysis buffer (50 mM Tris-HCl, 150 mM NaCl, 5 mM EDTA, 1% Triton X-100, 1 mM sodium fluoride, 1 mM sodium vanadate, and 1% deoxycholate) supplemented with protease inhibitors. After centrifugation at 15,000 *g* for 10 min, The protein concentration in the supernatant was determined using the DC protein assay kit (Bio-Rad, CA), Proteins were then boiled in SDS sample buffer for 5 min, subjected to 10% SDS-PAG, and transferred onto a polyvinylidene difluoride membrane (Millipore,

Billerica, MA). The membrane was probed with the indicated primary antibody, washed three times for 30 min, incubated with secondary antibody conjugated to horseradish peroxidase (HRP) for 2 h, and washed three times for 30 min. Blots were developed using SuperSignal West Femto Maximum Sensitivity Substrate (Pierce, Rockford, IL), and visualized with a LAS-3000 luminescent image analyzer (Fuji Photo Film Co., Tokyo, Japan). Antibodies against c-Fos, NFATc1 and actin were purchased from Santa Cruz Biotechnology (Dallas, TX). Antibody against $KCNK1$ was purchased from Abcam. All others antibodies were obtained from Cell Signaling Technology (Beverly, MA). Actin was used as a loading control.

Retroviral study
The coding sequence of the $KCNK1$ gene was prepared by RT-PCR with the following primers: $KCNK1$ forward primer with BamHI site, 5′-GCT-AGGATCCATGCTGCAGTCCCTGGCCGGCA-3′; $KCNK1$ reverse primer with NotI site, 5′-GCTAGCGGCCGCGTGGTCTGCAGAGCCA-TCC-3′. $KCNK1$ was cloned into the retroviral vector pMX-puro (Cell Biolabs, San Diego, CA). The forward shRNA oligonucleotides for sh-$KCNK1$ was 5′-GATCCCCGCAATTATGGAGTGTCGGTTTCAAGAG-AACCGACACTCCATAATTGCTTTTTC-3′, and the reverse was 5′-TCG-AGAAAAAGCAATTATGGAGTGTCGGTTCTCTTGAAACCGACACT-CCATAATTGCGGG-3′. The oligonucleotides were cloned into the retroviral siRNA vector pSuper-retro-Puro (OligoEngine, Seattle, WA). Retroviral packaging was performed by transfecting the plasmids into Plat-E cells using Lipofectamine 2000 (Invitrogen Life Technologies). Viral supernatant was collected from the culture medium 48 h after transfection. BMMs were incubated with viral supernatant in the presence of polybrene (10 µg/ml). After infection, BMMs were cultured overnight, detached using StemPro® Accutase® Cell Dissociation Reagent (Invitrogen Life Technologies, Carlsbad, CA), and further cultured with M-CSF (30 ng/ml) and puromycin (2 µg/ml) for 2 days. Puromycin-resistant BMMs then differentiated into osteoclasts in the presence of M-CSF (30 ng/ml) and RANKL for 4–5 days.

Patch-clamp recording
Extracellular fluid containing 117 mM NaCl, 5 mM KCl, 2.5 mM $CaCl_2$, 1.2 mM $MgCl_2$, 1.2 mM NaH_2PO_4, 25 mM $NaHCO_3$, and 11 mM glucose was used for the patch-clamp recording, and continually aerated with 95% O_2 and 5% CO_2 gas to maintain its pH at ∼7.4. The high K^+ solution was made by equimolar substitution of KCl for NaCl. The pH of pipette (internal) solution containing 150 mM K-Glu, 10 mM HEPES, 5 mM KCl, 0.1 mM EGTA and 2 mM Mg-ATP was adjusted to 7.2 by KOH. Using a gravity-fed perfusion system (BPS-4SG, Ala Scientific Instruments, Farmingdale, NY), complete exchange of solutions occurred within 30 s. To record procedures, BMM cells were transferred into a recording chamber (volume of chamber, 0.5 ml) mounted on an inverted microscope (CK-30, Olympus, Tokyo, Japan). Recording electrodes were prepared from capillary glass tubes (TW150-3, WPI, FL) using a microelectrode pipette puller (PP830, Narishige, Japan), and positioned using a micromanipulator (MPC-200, Sutter Instrument Co., Novato, CA). Patch pipettes filled with the pipette solutions were used at a resistance ranging from 5–8 MΩ. Membrane currents were recorded using Axopatch 200B amplifier (Axon Instruments, Union City, CA) that was connected to a computer using an analog-to-digital converter (Digidata 1322A, Axon Instruments). Currents recording and data analysis (n=10) were performed using pClamp software (Version 9.0, Axon Instruments). Generated currents were filtered with a low-pass eight-pole Bessel filter at 2 kHz. All experiments were performed at room temperature.

Intracellular Ca^{2+} measurement
BMMs were seeded at a density of 1×10^5 cells/well in a black clear 96-well plate and cultured in the presence of RANKL (10 ng/ml) and M-CSF (30 ng/ml) for 48 h. For measuring Ca^{2+} oscillations in individual osteoclast precursors, cells were loaded with 5 µM Fura-2-AM (Invitrogen Life Technologies) and 0.05% pluronic F127 (Sigma-Aldrich) for 30 min at room temperature. After washing three times with Dulbecco's modified Eagle's medium including 5.3 mM KCl (Gibco, Grand Island, NY) and

changed to Hank's balanced salt solution including 400 mg/ml KCl (Gibco), the fluorescence was recorded at every 2–3 s with 340 and 380 nm excitations and emitted through a 510-nm cut-off filter at 37°C using a BD pathway system (BD Biosciences, San Jose, CA) for 300 s. All results were digitized to the mean of the ratio (340 nm:380 nm).

Statistical analysis
All quantitative values are presented as mean±s.d. Each experiment was performed three to five times, and results from one representative experiment are shown. Statistical differences were analyzed using a Student's t-test. A value of $P<0.05$ was considered significant.

References
Arkett, S. A., Dixon, S. J. and Sims, S. M. (1992). Substrate influences rat osteoclast morphology and expression of potassium conductances. *J. Physiol.* **458**, 633-653.

Arrighi, I., Lesage, F., Scimeca, J.-C., Carle, G. F. and Barhanin, J. (1998). Structure, chromosome localization, and tissue distribution of the mouse twik K+ channel gene. *FEBS Lett.* **425**, 310-316.

Boyce, B. F. and Xing, L. (2008). Functions of RANKL/RANK/OPG in bone modeling and remodeling. *Arch. Biochem. Biophys.* **473**, 139-146.

Bucay, N., Sarosi, I., Dunstan, C. R., Morony, S., Tarpley, J., Capparelli, C., Scully, S., Tan, H. L., Xu, W., Lacey, D. L. et al. (1998). osteoprotegerin-deficient mice develop early onset osteoporosis and arterial calcification. *Genes Dev.* **12**, 1260-1268.

Chang, E.-J., Ha, J., Huang, H., Kim, H. J., Woo, J. H., Lee, Y., Lee, Z. H., Kim, J. H. and Kim, H.-H. (2008). The JNK-dependent CaMK pathway restrains the reversion of committed cells during osteoclast differentiation. *J. Cell Sci.* **121**, 2555-2564.

Choi, S.-W., Park, K.-I., Yeon, J.-T., Ryu, B. J., Kim, K.-J. and Kim, S. H. (2014). Anti-osteoclastogenic activity of matairesinol via suppression of p38/ERK-NFATc1 signaling axis. *BMC Complement Altern. Med.* **14**, 35.

Cummings, S. R. and Melton, L. J. (2002). Epidemiology and outcomes of osteoporotic fractures. *Lancet* **359**, 1761-1767.

Darnay, B. G., Haridas, V., Ni, J., Moore, P. A. and Aggarwal, B. B. (1998). Characterization of the intracellular domain of receptor activator of NF-kappaB (RANK). Interaction with tumor necrosis factor receptor-associated factors and activation of NF-kappab and c-Jun N-terminal kinase. *J. Biol. Chem.* **273**, 20551-20555.

Dempster, D. W., Compston, J. E., Drezner, M. K., Glorieux, F. H., Kanis, J. A., Malluche, H., Meunier, P. J., Ott, S. M., Recker, R. R. and Parfitt, A. M. (2013). Standardized nomenclature, symbols, and units for bone histomorphometry: a 2012 update of the report of the ASBMR Histomorphometry Nomenclature Committee. *J. Bone Miner. Res.* **28**, 2-17.

Enyedi, P. and Czirjak, G. (2010). Molecular background of leak K+ currents: two-pore domain potassium channels. *Physiol. Rev.* **90**, 559-605.

Espinosa, L., Paret, L., Ojeda, C., Tourneur, Y., Delmas, P. D. and Chenu, C. (2002). Osteoclast spreading kinetics are correlated with an oscillatory activation of a calcium-dependent potassium current. *J. Cell Sci.* **115**, 3837-3848.

Jimi, E., Akiyama, S., Tsurukai, T., Okahashi, N., Kobayashi, K., Udagawa, N., Nishihara, T., Takahashi, N. and Suda, T. (1999). Osteoclast differentiation factor acts as a multifunctional regulator in murine osteoclast differentiation and function. *J. Immunol.* **163**, 434-442.

Kajiya, H., Okamoto, F., Fukushima, H., Takada, K. and Okabe, K. (2003). Mechanism and role of high-potassium-induced reduction of intracellular Ca2+ concentration in rat osteoclasts. *Am. J. Physiol. Cell Physiol.* **285**, C457-C466.

Kelly, M. E. M., Dixon, S. J. and Sims, S. M. (1992). Inwardly rectifying potassium current in rabbit osteoclasts: a whole-cell and single-channel study. *J. Membr. Biol.* **126**, 171-181.

Kim, H.-H., Lee, D. E., Shin, J. N., Lee, Y. S., Jeon, Y. M., Chung, C.-H., Ni, J., Kwon, B. S. and Lee, Z. H. (1999). Receptor activator of NF-kappaB recruits multiple TRAF family adaptors and activates c-Jun N-terminal kinase. *FEBS Lett.* **443**, 297-302.

Lesage, F., Guillemare, E., Fink, M., Duprat, F., Lazdunski, M., Romey, G. and Barhanin, J. (1996). TWIK-1, a ubiquitous human weakly inward rectifying K+ channel with a novel structure. *EMBO J.* **15**, 1004-1011.

Lesage, F., Lauritzen, I., Duprat, F., Reyes, R., Fink, M., Heurteaux, C. and Lazdunski, M. (1997). The structure, function and distribution of the mouse TWIK-1 K+ channel. *FEBS Lett.* **402**, 28-32.

Negishi-Koga, T. and Takayanagi, H. (2009). Ca2+-NFATc1 signaling is an essential axis of osteoclast differentiation. *Immunol. Rev.* **231**, 241-256.

Nie, X., Arrighi, I., Kaissling, B., Pfaff, I., Mann, J., Barhanin, J. and Vallon, V. (2005). Expression and insights on function of potassium channel TWIK-1 in mouse kidney. *Pflugers Arch.* **451**, 479-488.

Rao, A., Luo, C. and Hogan, P. G. (1997). Transcription factors of the NFAT family: regulation and function. *Annu. Rev. Immunol.* **15**, 707-747.

Sato, K., Suematsu, A., Nakashima, T., Takemoto-Kimura, S., Aoki, K., Morishita, Y., Asahara, H., Ohya, K., Yamaguchi, A., Takai, T. et al. (2006). Regulation of osteoclast differentiation and function by the CaMK-CREB pathway. *Nat. Med.* **12**, 1410-1416.

Shevde, N. K., Bendixen, A. C., Dienger, K. M. and Pike, J. W. (2000). Estrogens suppress RANK ligand-induced osteoclast differentiation via a stromal cell independent mechanism involving c-Jun repression. *Proc. Natl. Acad. Sci. USA* **97**, 7829-7834.

Shibata, T., Sakai, H. and Nakamura, F. (1996). Membrane currents of murine osteoclasts generated from bone marrow/stromal cell co-culture. *Osaka City Med. J.* **42**, 93-107.

Sims, S. M. and Dixon, S. J. (1989). Inwardly rectifying K+ current in osteoclasts. *Am. J. Physiol.* **256**, C1277-C1282.

Srivastava, S., Weitzmann, M. N., Cenci, S., Ross, F. P., Adler, S. and Pacifici, R. (1999). Estrogen decreases TNF gene expression by blocking JNK activity and the resulting production of c-Jun and JunD. *J. Clin. Invest.* **104**, 503-513.

Takayanagi, H. (2007). Osteoimmunology: shared mechanisms and crosstalk between the immune and bone systems. *Nat. Rev. Immunol.* **7**, 292-304.

Takayanagi, H., Ogasawara, K., Hida, S., Chiba, T., Murata, S., Sato, K., Takaoka, A., Yokochi, T., Oda, H., Tanaka, K. et al. (2000). T-cell-mediated regulation of osteoclastogenesis by signalling cross-talk between RANKL and IFN-gamma. *Nature* **408**, 600-605.

Takayanagi, H., Kim, S., Koga, T., Nishina, H., Isshiki, M., Yoshida, H., Saiura, A., Isobe, M., Yokochi, T., Inoue, J.-I. et al. (2002). Induction and activation of the transcription factor NFATc1 (NFAT2) integrate RANKL signaling in terminal differentiation of osteoclasts. *Dev. Cell* **3**, 889-901.

Valverde, P., Kawai, T. and Taubman, M. A. (2004). Selective blockade of voltage-gated potassium channels reduces inflammatory bone resorption in experimental periodontal disease. *J. Bone Miner. Res.* **19**, 155-164.

Valverde, P., Kawai, T. and Taubman, M. A. (2005). Potassium channel-blockers as therapeutic agents to interfere with bone resorption of periodontal disease. *J. Dent. Res.* **84**, 488-499.

Vicente, R., Escalada, A., Coma, M., Fuster, G., Sanchez-Tillo, E., Lopez-Iglesias, C., Soler, C., Solsona, C., Celada, A. and Felipe, A. (2003). Differential voltage-dependent K+ channel responses during proliferation and activation in macrophages. *J. Biol. Chem.* **278**, 46307-46320.

Yang, S. and Li, Y.-P. (2007). RGS10-null mutation impairs osteoclast differentiation resulting from the loss of [Ca2+]i oscillation regulation. *Genes Dev.* **21**, 1803-1816.

Zhou, M., Xu, G., Xie, M., Zhang, X., Schools, G. P., Ma, L., Kimelberg, H. K. and Chen, H. (2009). TWIK-1 and TREK-1 are potassium channels contributing significantly to astrocyte passive conductance in rat hippocampal slices. *J. Neurosci.* **29**, 8551-8564.